the abruptly decreased isomer shift and narrow linewidth of the Mössbauer spectrum and the low Néel temperature at the composition of $x=1.34$.

Conclusion

Solid solutions of all the compositions have brownmillerite structure. The Al^{3+} ion with the smaller ionic radius prefers the tetrahedral site but the preference decreases at the increased x value. The Al^{3+} and Fe^{3+} ions are randomly distributed in each octahedral and tetrahedral sites. The substitution of diamagnetic Al^{3+} ion in place of paramagnetic Fe^{3+} ion decreases the exchange integral. The Fe^{3+} ion is isolated by diamagnetic ions at the composition of $x=1.34$ and the composition has no long range ordering of Fe^{3+} ion spins above 5 K. The composition of $x=1.34$ may be below the percolation threshold of a Heisenberg antiferromagnet. The Fe^{3+} ion is high spin state and thus isotropic. The spin direction can be changed by local anisotropic field in the compositions of $x=0.00$-0.66 with space group of *Pcmn*. However the compositions of $x=1.00$ and 1.34 do not show spin reorientation when cooling due to high symmetric space group of *Ibm2*.

Acknowledgment. This work was supported by grant No. 92-25-00-02 from the Korea Science and Engineering Foundation in 1993 and therefore we express our appreciation to the authorities concerned.

References

1. Büssem, *Fortschr. Min.* **1937**, *22*, 31.
2. Colville, A. A. *Acta Cryst.* **1970**, *B26*, 1469.
3. Battle, P. D.; Bollen, S. K.; Gibb, T. C.; Matsuo, M. *J. Solid State Chem.* **1990**, *90*, 42.
4. Geller, S.; Grant, R. W.; Fullmer, I. D. *J. Phys. Chem. Solids* **1970**, *31*, 793.
5. Battle, P. D.; Gibb, T. C.; Lightfoot, P. *J. Solid State Chem.* **1988**, *76*, 334.
6. Smith, D. K. *Acta Cryst.* **1962**, *15*, 1146.
7. Shin, S.; Yonemura, M.; Ikawa, H. *Bull. Chem. Soc. Japan* **1979**, *52*, 947.
8. Gibb, T. C. *J. Chem. Soc., Dalton Trans.* **1983**, 873.
9. Grenier, J. C.; Fournés, L. *Mat. Res. Bull.* **1982**, *17*, 55.
10. Gibb, T. C. *J. Solid State Chem.* **1990**, *88*, 485.
11. Gibb, T. C. *J. Chem. Soc., Dalton Trans.* **1983**, 2031.
12. Grenier, J. C.; Pouchard, M. *J. Solid State Chem.* **1975**, *13*, 92.
13. Rodriguez, R.; Frenández, A.; Isalgué, A.; Rodriguez, J.; Labarta, A.; Teiada, J.; Obradors, X. *J. Phys. C: Solid State Phys.* **1985**, *18*, L 401.
14. Yo, C. H.; Lee, E. S.; Pyon, M. S. *J. Solid State Chem.* **1988**, *73*, 411.
15. Yo, C. H.; Kim, H. R.; Ryu, K. H.; Roh, K. S.; Choy, J. H. *Bull. Kor. Chem. Soc.* **1994**, *15*, 636.

Hydrolysis of *p*-Nitrophenyl Acetate and *p*-Nitrophenyldiphenyl Phosphate in Micellar Solution by *N*-Chloro Compounds: Involvement of Counter Ions in Micellar Catalysis

Byeong-Deog Park[†] and Yoon-Sik Lee*

Department of Chemical Technology, Seoul National University, Seoul 151-742, Korea
[†]Aekyung Ind. Co., LTD., Central Research Lab., Taejon 300-200, Korea
Received June 24, 1995

Hydrolysis of *p*-nitrophenyl acetate (PNPA) and *p*-nitrophenyldiphenyl phosphate (PNPDPP) by *N*-chloro compounds in micellar solution were studied. *N,N'*-Dichloroisocyanuric acid sodium salt (DCI) in cetyltrimethylammonium chloride (CTACl) micellar solution gave pseudo first-order kinetics. But, DCI in cetyltrimethylammonium bromide (CTABr) micellar solution showed typical series first-order kinetics - fast hydrolysis of the esters and concomitant slow decay of the hydrolyzed product, *p*-nitrophenolate. The hydrolysis rate was decreased as the hydrophobicity of *N*-chloro compounds was increased, which is the opposite trend to the usual bimolecular micellar reaction. This curious behavior of the *N*-chloro compounds in the catalytic hydrolysis of PNPA and PNPDPP in a cationic micellar system can be best explained by participation of counter ions of the surfactants during hydrolysis.

Introduction

As a mimic system of enzyme catalysis and a model system for destruction of nerve agents, the hydrolysis of *p*-nitrophenyl acetate (PNPA) and *p*-nitrophenyldiphenyl phosphate (PNPDPP) in either micellar or microemulsion system has been extensively investigated.[1] We had previously reported some interesting results of the hydrolysis of PNPA by *N,N'*-dichloroisocyanuric acid sodium salts (DCI) in cationic micellar system.[2] In that paper, we concluded that the difference in the reactivity of the catalytic hydrolysis of PNPA by DCI in various cationic micellar systems were due to formation of different halogen species which were formed by the reaction between the counter ions of the surfactant

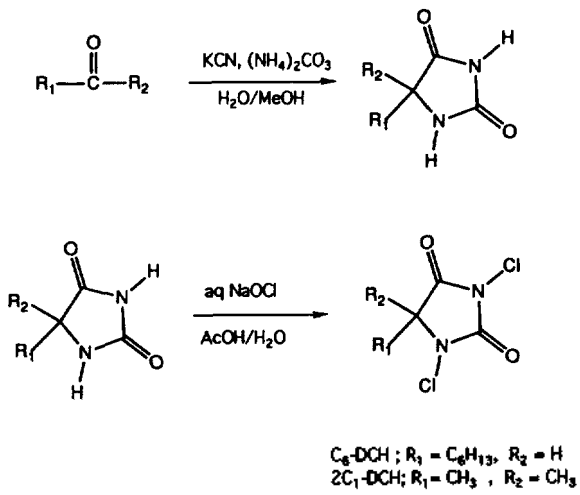

Scheme 1. Preparation of *N*-chlorohydantoin derivatives ($2C_1$-DCH and C_6-DCH).

and DCI.

In similar studies concerning the chlorination of phenol by *N*-chloro compounds in CTACl micelle, we previously reported that the *o/p* selectivity was controlled by the concentration of surfactant. Even bromophenols became major products when the surfactant concentration was very high above CMC.[3] We also proposed that these results were due to the halogen species formed in the Stern layer of the micelle.

We now wish to report the results of the hydrolysis of PNPA and PNPDPP catalyzed by various *N*-chloro compounds which have different hydrophobicity. Varying the hydrophobicity of the *N*-chloro compounds, their catalytic behavior in the micellar phase is changed. From these results, we wish to confirm the previously proposed mechanisms.

Results and Discussions

The hydantoin derivatives, 5,5-dimethylhydantoin and 5-hexylhydantoin, were synthesized by Bucherer's method[4] from the reaction between acetone and heptanal according to Scheme 1.

These hydantoin derivatives showed characteristic IR peaks at 3150, 1720, 1440 cm^{-1} respectively. Chlorination of the hydantoin derivatives by aq. NaOCl solution yielded *N,N'*-dichloro-5,5-dimethylhydantoin ($2C_1$-DCH) and *N,N'*-dichloro-5-hexylhydantoin (C_6-DCH). After the chlorination reactions, N-H stretching peak at 3150 cm^{-1} was disappeared completely. *N*-Butylisocyanuric acid was prepared from the reaction of cyanuric acid potassium salt and butyl bromide in dimethylsulfoxide (DMSO) solution. After treating with aq. NaOCl solution, it produced *N*-butyl-*N',N''*-dichloroisocyanuric acid (C_4-DCI) according to Scheme 2.

The chlorinations were carried out in a mild acidic medium such as acetic acid. Otherwise, the reactions would have been very sluggish. The chlorinations were done just before the hydrolysis reactions, and only freshly made *N*-chloro compounds were used in the kinetic study. The stock solutions of PNPA and PNPDPP were prepared from dry dioxane. The stock solution of DCI was prepared from distilled water, while those of other *N*-chloro compounds were

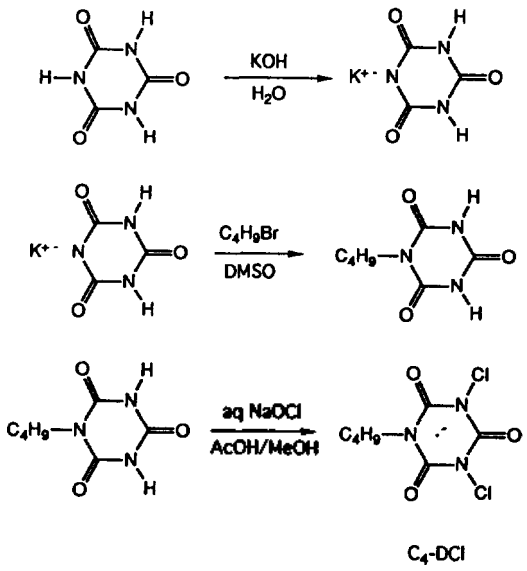

Scheme 2. Preparation of *N,N'*-dichloro-*N''*-butylisocyanuric acid (C_4-DCI).

Table 1. Rate Constants for the Hydrolysis of PNPA by *N,N'*-Dichloroisocyanuric Acid Sodium Salts (DCI) in Micellar Solution[a]

Entry	Surfactant	Catalyst	k_1 (s^{-1})	k_2[b] (s^{-1})	k_1^{cat} ($M^{-1}s^{-1}$)	k_1/k_0
1	CTABr[c]	DCI	5.1×10^{-2}	1.1×10^{-2}	42.5	2040
2	CTACl	DCI	7.6×10^{-3}		6.3	304
3	CTABr	none	1.0×10^{-4}			4
4	none	DCI	6.1×10^{-3}		5.1	240
5	none	none	2.5×10^{-5}			1

[a]Conditions: pH 8.0, 0.05 M phosphate buffer, 25± 0.1 ℃, [DCI] $=1.2\times10^{-3}$ M, [PNPA] $=4\times10^{-5}$ M, [Surfactant] $=4\times10^{-3}$ M. Calculated by pseudo first-order kinetics for the release of *p*-nitrophenolate ion, monitored at 400 nm. Reproducibilities of the rate constants are $<\pm5\%$. [b]The rate for the decay of *p*-nitrophenolate. [c]Calculated by series first-order kinetics equation.[5]

prepared from dry dioxane. Reactions were initiated by injecting the substrate stock solution into micellar surfactant solution which contained a fixed amount of the catalyst. Hydrolysis were monitored at 400 nm from the release of 4-nitrophenolate. The kinetic data for the hydrolysis of PNPA are summarized in Table 1.

In nonmicellar phase, DCI showed rate enhancement with 240-fold over the system without DCI (entry 4). This means that DCI itself is a strong catalyst in the hydrolysis of PNPA. In the micellar phase of CTACl, DCI gave a 304-fold rate enhancement (entry 2). Comparing with entry 4, the micellar catalytic effect by CTACl was very small. But in the micellar phase of CTABr, DCI showed a 2040-fold rate enhancement (entry 1), which means that the reactivity of DCI is increased by a factor of 6.5 in CTABr micellar phase. In addition, the CTABr micellar system showed quite a different kind of kinetic behavior from the previous ones. Instead of pseudo

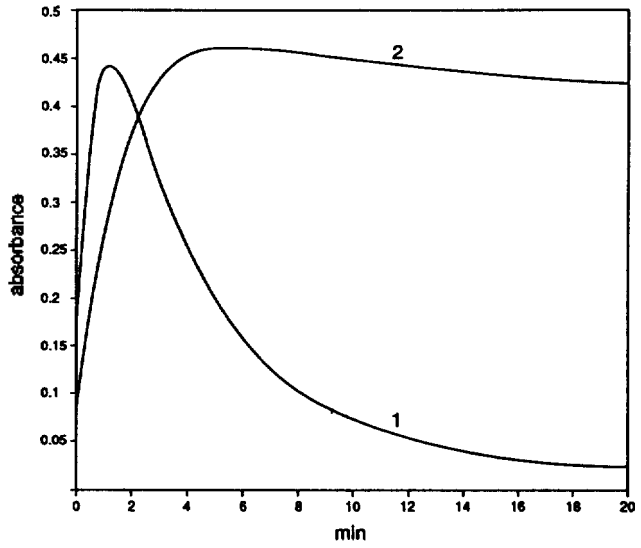

Figure 1. Relative absorbances at 400 nm during cleavage of PNPA by DCI in CTABr and CTACl micellar solution, 1; CTABr, 2; CTACl. Condition: pH 8.0, 0.05 M phosphate buffer, 25± 0.1 ℃, [DCI]=1.2×10^{-3} M, [PNPA]=4×10^{-5} M, [Surfactant]=4×10^{-3} M.

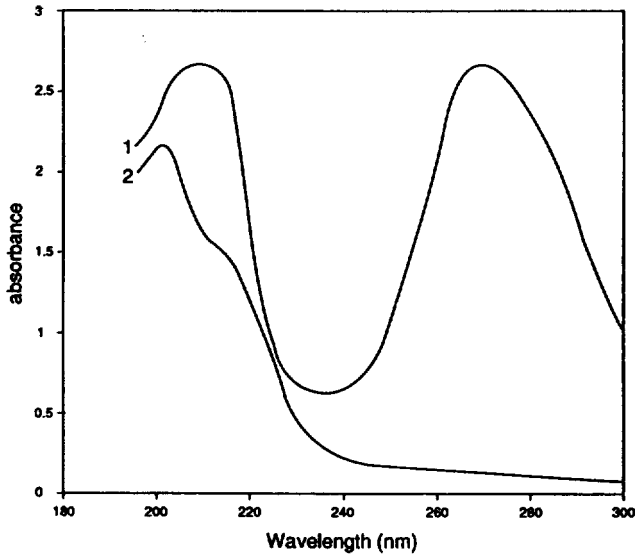

Figure 2. UV spectra of DCI in CTABr and CTACl micellar solution, 1; CTABr, 2; CTACl. Condition: pH 8.0, 0.05 M phosphate buffer, 25± 0.1 ℃, [DCI]=1.2×10^{-3} M, [Surfactant]=4×10^{-3} M.

first-order kinetics, it showed typical series first-order kinetics[5]-fast hydrolysis of esters and the concomitant slow decay of the hydrolysis product, *p*-nitrophenolate. Under the hydrolysis condition, it seemed that *p*-nitrophenolate was rapidly transformed to other compounds which did not have λ_{max} at 400 nm (Figure 1).

The possible products might be multi-halogenated *p*-nitrophenolates, which have low extinction coefficients around 400 nm.[6] In a separate experiment, after 96 mmol of DCI was reacted with 45 mmol of *p*-nitrophenolate in 150 mL of CTABr (100 mM) solution for 40 min. at room temperature, 2,6-dibromo-4-nitrophenol was isolated in 9% yield. The successive halogenation can ultimately lead the *p*-nitrophenolates to a ring rupture pathway, giving off volatile halogenated hydrocarbons. Similar ring rupture reactions of aromatic compounds in chlorination reactions had been previously reported.[7] As a result of this, the hydrolysis of PNPA in a CTABr micellar solution showed a typical series first-order kinetics.

When 20 μL of DCI stock solution was added to 3 mL of CTABr (4 mM) micellar solution which did not contain PNPA, a strong absorbance appeared at 264 nm region which is identical to that of Br_3^- ion. (λ_{max} lit.[8] 266 nm, ε 35,000 M^{-1} cm^{-1}). On the contrary, DCI in CTACl micellar solution did not reveal any noticeable peak from 240 nm to 300 nm (Figure 2). From the absorbance value, the mole fraction of Br_3^- to DCI was calculated to be about 11%.

The formation of Br_3^- ion[9] can be easily conjectured if the reaction between DCI and the bromide ion of the surfactant yielded BrCl (Scheme 3). This reaction is an oxidation of the bromide ion by DCI. The initial product, BrCl, is very unstable in aqueous solution. Thus, it is easily hydrolyzed to chloride ion and HOBr, which can be further equilibrated with various bromine species.[9] Among these bromine species, Br_3^- ion is known to be relatively stable.[9]

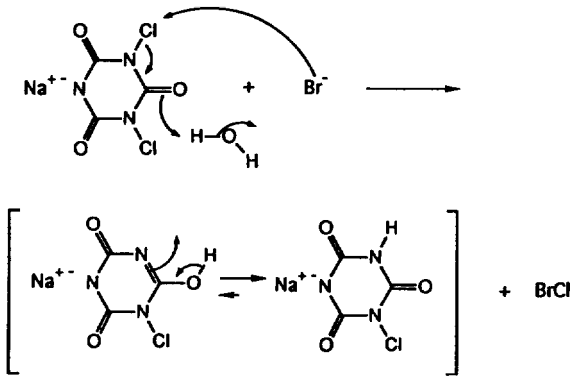

Scheme 3. The oxidation reaction of bromide by DCI.

When PNPA was injected to the DCI in CTABr solution, the absorbance at 264 nm was sharply decreased by about 20% (Figure 3). But, we could not observe any further changes in the absorbance of Br_3^- after about 5 seconds. This indicates that certain amounts of Br_3^- was rapidly consumed in one way or another during the initial period of the reaction. In aromatic halogenation or addition reaction of alkenes, the bromine species such as BrCl, Br_2 or Br_3^- ion were known to be more reactive than *N*-chloro compounds.[10] Accordingly, these bromine species can be added to the aromatic rings of PNPA or act as a Lewis acid catalyst on the carbonyl group of PNPA during the hydrolysis[11] (Scheme 4).

When the CTABr concentration was increased, the hydrolysis of PNPA by DCI was increased linearly (Figure 4). Under the same condition without PNPA, the concentration of Br_3^- ion was also increased linearly (Figure 5). Accordingly, the rate enhancement in the CTABr micellar solution closely related to the formation of Br_3^-. These results also support that the bromine species play an important role in PNPA

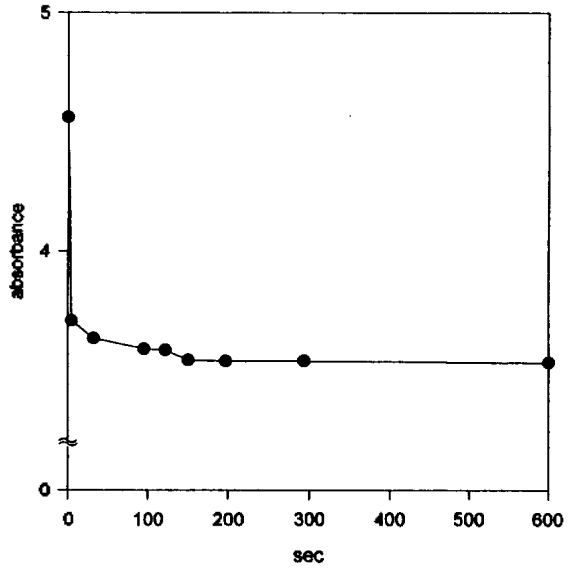

Figure 3. Relative absorbances at 266 nm after adding PNPA to CTABr micellar solution containing DCI. Condition: pH 8.0, 0.05 M phosphate buffer, 25± 0.1 ℃, [DCI]=1.2×10^{-3} M, [PNPA]=4×10^{-5} M, [CTABr]=4×10^{-3} M.

Path 1

Path 2

Path 3

Scheme 4. Possible reaction pathway in the hydrolysis of PNPA by DCI in CTABr micelle.

hydrolysis.

In the CTACl micellar solution, the same reaction between the DCI and chloride counter ion might have a chance to yield chlorine and various chlorine species. But these chlorine species were known to be less reactive than bromine species in aromatic halogenation or addition reaction in alkene.[10] In addition, when the UV spectra were taken, no significant amount of chlorine species[8] such as OCl^- could be detected (Figure 2, Figure 5). Unlike the CTABr micellar solution, the hydrolysis reaction of PNPA by DCI in the CTACl micellar solution showed typical saturation type ki-

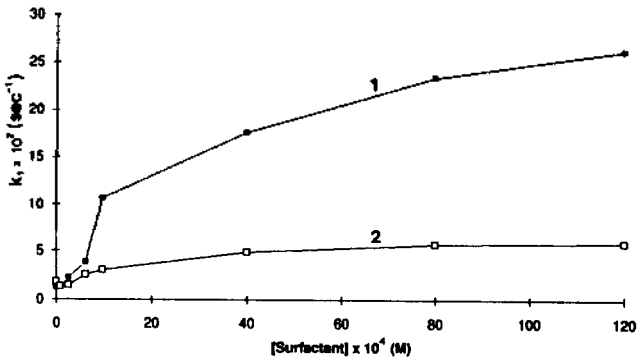

Figure 4. Hydrolysis rate constant of PNPA *vs.* surfactant concentration, 1; CTABr, 2; CTACl. Condition: pH 8.6, 0.05 M phosphate buffer, 25± 0.1 ℃, [DCI]=1.2×10^{-3} M, [PNPA]=4×10^{-5} M.

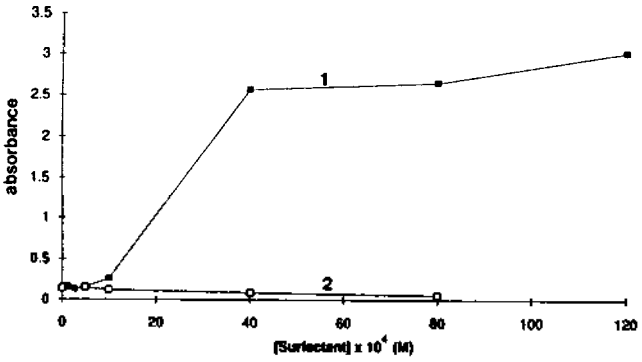

Figure 5. Relative absorbances at 266 nm (for 1) and 292 nm (for 2) of halogen species *vs.* surfactant concentration, 1; CTABr, 2; CTACl. Condition: pH 8.58, 0.05 M phosphate buffer, 25± 0.1 ℃, [DCI]=1.2×10^{-3} M.

netics as the concentration of surfactant was increased. This result indicates that the hydrolysis reaction by DCI in the CTACl micellar solution is a simple micellar reaction.

If one of the cascades of the catalytic hydrolysis in the CTABr micellar solution begins by the formation of BrCl from DCI and bromide ion in the Stern layer, the hydrophobicity of the catalyst or the substrate will exert some effect upon the hydrolysis reactions. To see the effects of the hydrophobicity of the catalysts on the hydrolysis reactions, the rate constants for the hydrolysis of PNPA by various *N*-chloro compounds which have different hydrophobicity are measured and the results are summarized in Table 2.

Without exception, all the hydrophobic *N*-chloro compounds are less active than the hydrophilic *N*-chloro compound, DCI, in the hydrolysis of PNPA. In addition, the DCH derivatives even revealed pseudo first-order kinetics. Thus, the most hydrophobic *N*-chloro compound, C_6-DCH gave only 176-fold rate enhancement. It is even a smaller value than that of DCI in the buffer system. As the reactions are accelerated mainly by the bromine species, it is reasonable that the hydrophobic *N*-chloro compounds showed less reactivity in micellar systems. It is because the relative positions of the hydrophobic *N*-chloro compounds such as C_6-DCH, $2C_1$-DCH, C_4-DCI in micellar phase are near the micelle core, where those *N*-chloro compounds have a little chance to

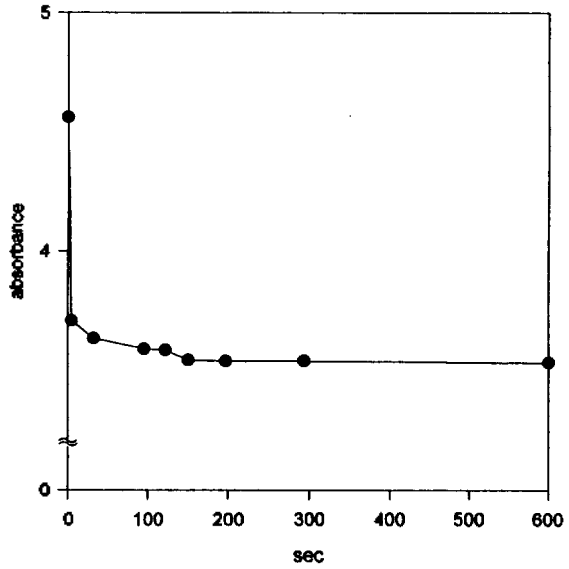

Figure 3. Relative absorbances at 266 nm after adding PNPA to CTABr micellar solution containing DCI. Condition: pH 8.0, 0.05 M phosphate buffer, 25± 0.1 ℃, [DCI]=1.2×10^{-3} M, [PNPA]=4×10^{-5} M, [CTABr]=4×10^{-3} M.

Path 1

Path 2

Path 3

Scheme 4. Possible reaction pathway in the hydrolysis of PNPA by DCI in CTABr micelle.

hydrolysis.

In the CTACl micellar solution, the same reaction between the DCI and chloride counter ion might have a chance to yield chlorine and various chlorine species. But these chlorine species were known to be less reactive than bromine species in aromatic halogenation or addition reaction in alkene.[10] In addition, when the UV spectra were taken, no significant amount of chlorine species[8] such as OCl^- could be detected (Figure 2, Figure 5). Unlike the CTABr micellar solution, the hydrolysis reaction of PNPA by DCI in the CTACl micellar solution showed typical saturation type ki-

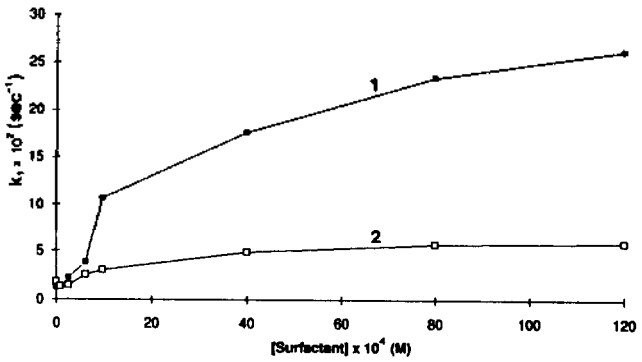

Figure 4. Hydrolysis rate constant of PNPA *vs.* surfactant concentration, 1; CTABr, 2; CTACl. Condition: pH 8.6, 0.05 M phosphate buffer, 25± 0.1 ℃, [DCI]=1.2×10^{-3} M, [PNPA]=4×10^{-5} M.

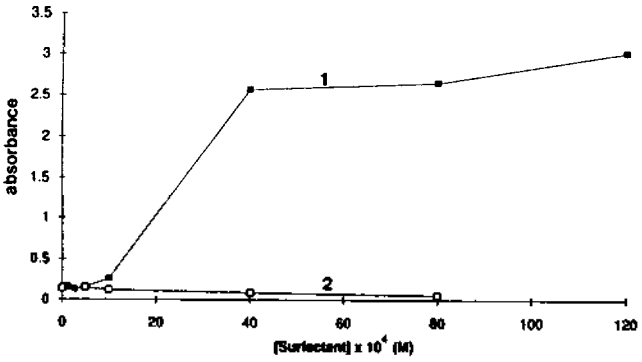

Figure 5. Relative absorbances at 266 nm (for 1) and 292 nm (for 2) of halogen species *vs.* surfactant concentration, 1; CTABr, 2; CTACl. Condition: pH 8.58, 0.05 M phosphate buffer, 25± 0.1 ℃, [DCI]=1.2×10^{-3} M.

netics as the concentration of surfactant was increased. This result indicates that the hydrolysis reaction by DCI in the CTACl micellar solution is a simple micellar reaction.

If one of the cascades of the catalytic hydrolysis in the CTABr micellar solution begins by the formation of BrCl from DCI and bromide ion in the Stern layer, the hydrophobicity of the catalyst or the substrate will exert some effect upon the hydrolysis reactions. To see the effects of the hydrophobicity of the catalysts on the hydrolysis reactions, the rate constants for the hydrolysis of PNPA by various *N*-chloro compounds which have different hydrophobicity are measured and the results are summarized in Table 2.

Without exception, all the hydrophobic *N*-chloro compounds are less active than the hydrophilic *N*-chloro compound, DCI, in the hydrolysis of PNPA. In addition, the DCH derivatives even revealed pseudo first-order kinetics. Thus, the most hydrophobic *N*-chloro compound, C_6-DCH gave only 176-fold rate enhancement. It is even a smaller value than that of DCI in the buffer system. As the reactions are accelerated mainly by the bromine species, it is reasonable that the hydrophobic *N*-chloro compounds showed less reactivity in micellar systems. It is because the relative positions of the hydrophobic *N*-chloro compounds such as C_6-DCH, $2C_1$-DCH, C_4-DCI in micellar phase are near the micelle core, where those *N*-chloro compounds have a little chance to

Table 2. Rate Constants for the Hydrolysis of PNPA by Various *N*-Chloro Compounds in CTABr Micellar Solution[a]

Surfactant	Catalyst	k_1 (s^{-1})	k_2[b] (s^{-1})	k_1^{cat} ($M^{-1}s^{-1}$)	k_1/k_0
CTABr[c]	DCI	5.1×10^{-2}	1.1×10^{-2}	42.5	2040
CTABr[c]	C_4-DCI	2.6×10^{-2}	1.5×10^{-3}	22	1040
CTABr	$2C_1$-DCH	7.5×10^{-3}		6.3	300
CTABr	C_6-DCH	4.4×10^{-3}		4	176
CTABr	none	1.0×10^{-4}			4
none	none	2.5×10^{-5}			1

[a]Conditions: pH 8.0, 0.05 M phosphate buffer, 25± 0.1 ℃, [Catalyst]=1.2×10^{-3} M, [PNPA]=4×10^{-5} M, [Surfactant]=4×10^{-3} M. Calculated by pseudo first-order kinetics for the release of *p*-nitrophenolate ion, monitored at 400 nm. Reproducibilities of the rate constants are <± 5%. [b]The rate for the decay of *p*-nitrophenolate. [c]Calculated by series first-order kinetics equation.[5]

Table 3. Rate Constants for the Hydrolysis of PNPDPP by *N,N'*-Dichloroisocyanuric Acid Sodium Salts (DCI) in Micellar Soultion[a]

Surfactant	Catalyst	k_1 (s^{-1})	k_2[b] (s^{-1})	k_1^{cat} ($M^{-1}s^{-1}$)	k_1/k_0
CTABr[c]	DCI	1.0×10^{-2}	7.1×10^{-3}	8.5	2000
16-OH[c]	DCI	7.6×10^{-3}	7.8×10^{-3}	6.5	1520
16-OH	none	1.2×10^{-3}			240
CTABr	none	6.0×10^{-4}			120
none	DCI	4.8×10^{-4}			96
none	none	5.0×10^{-6}			1

[a]Conditions: pH 8.0, 0.05 M phosphate buffer, 25± 0.1 ℃, [DCI]=1.2×10^{-3} M, [PNPDPP]=4×10^{-5} M, [Surfactant]=4×10^{-3} M. Calculated by pseudo first-order kinetics for the release of *p*-nitrophenolate ion, monitored at 400 nm. Reproducibilities of the rate constants are <± 5%. [b]The rate for the decay of *p*-nitrophenolate. [c]Calculated by series first-order kinetics equation.[5]

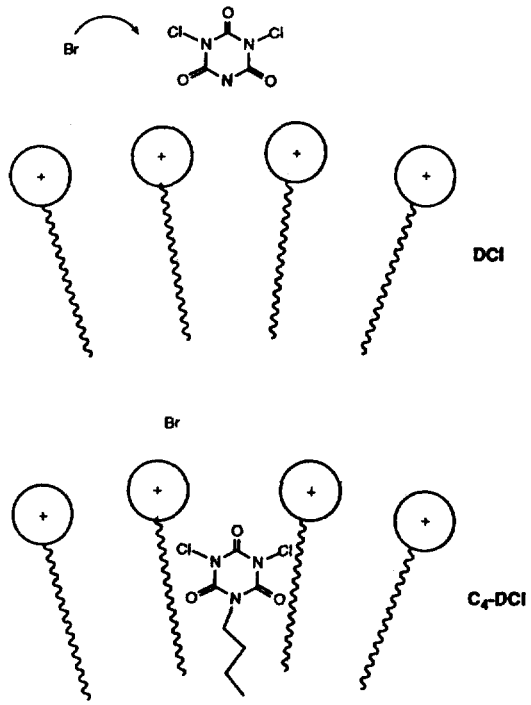

Scheme 5. Schematic representation of orientation of *N*-chloro compounds in micelle.

react with the bromide counter ion for the formation of bromine species (Scheme 5).

The hydrophobicity of $2C_1$-DCH is less than that of C_6-DCH, which means that $2C_1$-DCH located near the Stern layer in the micellar phase. As a result, $2C_1$-DCH gave a 300-fold rate enhancement, which is higher than that of C_6-DCH (176). On the other hand, $2C_1$-DCH showed lower reactivity than that of C_4-DCI (1040). By the same trend, it is expected that the reactivity of $2C_1$-DCH would be higher than that of C_4-DCI, because the hydrophobicity of C_4-DCI may look greater than that of $2C_1$-DCH. This result can be explained by the structural differences of the *N*-chloro compounds. The DCI derivatives have two chlorites, which are all on the imide position. But, the DCH derivatives have one chlorite on the imide position and the other on the amide position, and the latter has a lower reactivity than the former.

The rate constants for the hydrolysis of PNPDPP by DCI in cationic micellar surfactant solutions are summarized in Table 3. The results of PNPDPP which is more hydrophobic substrate than PNPA can be explained similarly. Generally, as the hydrophobicity of an ester substrate is increased in micellar systems, the hydrolysis rate is increased due to a stronger binding to the micelle.[12] Thus, in CTABr micellar systems without DCI, the rate enhancement of PNPDPP is 120-fold, while that of PNPA is only 4. Therefore, it was expected that DCI would give a higher rate enhancement with PNPDPP than with PNPA. But, DCI only revealed a similar rate enhancement (2000) as in the hydrolysis of PNPA (2040). Comparing to the hydrolysis of PNPA, a noticeable rate enhancement was not observed in the hydrolysis of PNPDPP, which can be located at the micellar phase with stronger binding. This also suggests that the formation of the bromine species is one of the key factors for the catalytic activity of the *N*-choro compounds in CTABr micellar system.

In conclusion, the differences in reactivity of the catalytic hydrolysis of esters by *N*-chloro compounds in cationic micellar systems are due to the formation of various halogen species during the hydrolysis reactions. Because the catalytic activity of active halogen species formed in the CTABr micellar phase is greater than that formed in the CTACl micellar system, a much faster rate was observed in the CTABr micellar solution. As far as we know, this will be the first report that clearly demonstrates the importance of counter ions in catalytic reactions in a micellar system. Because the relative positions of the hydrophobic *N*-chloro compounds such as C_6-DCH, $2C_1$-DCH, C_4-DCI in a micellar system is near the micelle core, they have less chances of forming bromine species by reacting with bromide counter ions. Therefore, they showed less reactivity than the hydrophilic *N*-chloro compound, DCI.

Experimental

The melting points were measured on a Yanaco MP-S5 and are uncorrected. *N,N'*-Dichloroisocyanuric acid sodium salts (DCI) was purchased from Aldrich Co. Other chemicals were reagent grade and purified prior to use. The IR spectra were obtained by a Jasco DS-710 IR spectrophotometer and the proton NMR spectra were recorded on a Jeol JNM-MH-100 NMR spectrometer. Elemental analyses were performed with a Yanaco MT-2 CHN corder. The ultraviolet absorption spectra were measured on a Shmadzu MPS-500. The analytical thin layer chromatography was performed on a silica gel plate (0.25 mm, 60F-254, E. Merck) with various solvent systems.

Cyanuric acid potassium salt. Cyanuric acid (5 g, 174 mmol) was dissolved in 200 mL of distilled water, and then slightly warmed to 80 ℃. After 2.2 g of KOH (39 mmol) in 25 mL of distilled water was added portionwise to the cyanuric acid solution, the solution was cooled in an ice bath. The resulting white precipitate was collected, washed with cold water, and dried. Yield 92%, mp>280 ℃.

***N*-Butylisocyanuric acid.** Butyl bromide (10.55 g, 770 mmol) was slowly added with magnetic stirring to a solution of cyanuric acid potassium salt (6.67 g, 385 mmol) in 70 mL of DMSO at 55 ℃ in a water bath. After 48 hours, 50 mL of distilled water was added into the solution, and the product was extracted by ether (50 mL×4). The ether solution was dehydrated by magnesium sulfate, and evaporated to yield white crude product. Several recrystallization from hexane afforded pure product (1.7 g, 24%). mp 219-221 ℃; TLC, Rf, 0.3 ($CHCl_3$: MeOH = 10 : 1, v/v); NMR (DMSO-d_6) δ 0.95 (t, 3H), 1.1-2.0 (m, 6H), 11.50 (s, 2H).

***N*-Butyl-*N'*,*N''*-dichloroisocyanuric acid (C_4-DCI).** Aqueous NaOCl (10% active chlorine, 9.7 mL) was slowly added dropwise with magnetic stirring to a solution of *N*-butylisocyanuric acid (1.8 g, 9.67 mmol) in 40 mL of MeOH and 20 mL of AcOH at room temperature. After the complete addition of NaOCl, the resulting white precipitate was filtered off. The residual solution was allowed to cool to −15 ℃. The resulting white needle crystals were collected, rinsed with cold distilled water and dried to yield 0.92 g (37%). mp 67-71 ℃; NMR ($CDCl_3$) δ 1.00 (t, 3H), 1.1-2.0 (m, 6H). Anal. Calcd. for $C_7H_9N_3O_3Cl_2$ (254.07): C 33.10; H 3.60; N 16.50%. Found: C 32.39; H 3.44; N 16.41%.

Hexylhydantoin. Heptanal (10 g, 87.5 mmol) was slowly added with magnetic stirring to a solution of KCN (11.41 g, 175 mmol), ammonium carbonate (39.9 g, 349.7 mmol) in 120 mL of ethanol and 80 mL of distilled water at 53 ℃ in a water bath. After 18 hours, the solution was evaporated to 70 mL at reduced pressure and cooled to 5 ℃. The yellow precipitate was filtered and rinsed with hexane. The product was recrystallized twice from EtOH, yielding 7.3 g (43%) of pure product. mp 142-145 ℃; TLC, 0.3 ($CHCl_3$: MeOH = 15 : 1, v/v); NMR (DMSO-d_6), δ 0.96 (t, 3H), 1.32 (s, 8H), 1.62 (m, 2H), 4.10 (t, 1H), 8.08 (s, 1H), 10.66 (s, 1H). Anal. Cacld. for $C_9H_{15}N_2O_2$ (183.23) : C 58.99; H 8.25; N 15.28%. Found: C 58.31; H 8.27; N 14.88%.

***N,N'*-Dichloro-5-hexylhydantoin (C_6-DCH).** Aqueous NaOCl (10% active chlorine, 45 mL) was added dropwise with magnetic stirring to a solution of hexylhydantoin (1.4 g, 7.59 mmol) in 50 mL of MeOH and 10 mL of AcOH at room temperature. After the complete addition of NaOCl, the resulting white precipitate was filtered off, and the filtrate was allowed to cool to −15 ℃. The resulting white needle crystals were collected, rinsed with cold distilled water, and dried to yield 0.77 g (40%). mp 31-33 ℃; NMR ($CDCl_3$), δ 0.95 (t, 3H), 1.36 (s, 8H), 2.0 (m, 2H), 4.20 (t, 1H). Anal. Cacld. for $C_9H_{14}N_2O_2Cl_2$ (253.13): C 42.71; H 5.58; N 11.07%. Found: C 43.30; H 5.49; N 11.41%.

5,5-Dimethylhydantoin. Acetone (2 g, 34.43 mmol) was added dropwise with magnetic stirring to a solution of KCN (4.48 g, 68.86 mmol), ammonium carbonate (15.71 g, 137.7 mmol) in 50% aqueous MeOH at 60 ℃ in a water bath. After 3 hours, the solution was evaporated to 60 mL at a reduced pressure and allowed to cool to room temperature. After the pH of the solution was adjusted to 6.0 by 3 N HCl, a white precipitate was formed. It was filtered and recrystallized in EtOH to yield 3.22 g (73%). mp 170-171 ℃; TLC, Rf 0.5 ($CHCl_3$: MeOH = 15 : 1, v/v); NMR (DMSO-d_6), δ 1.30 (s, 6H), 7.90 (broad, 1H).

***N,N'*-Dichloro-5,5-dimethylhydantoin ($2C_1$-DCH).** Aqueous NaOCl (10% active chlorine, 35 mL) was added dropwise with magnetic stirring to a solution of 5,5-dimethylhydantoin (2 g, 10 mmol) in 60 mL of 25% aqueous AcOH at room temperature. As soon as NaOCl was added, a white precipitate started to form. After 1 hour, the resulting white crystals were filtered, rinsed with cold distilled water and dried to get 1.4 g (70%). mp 129-130 ℃; TLC, Rf 0.8 ($CHCl_3$: MeOH = 15 : 1, v/v); NMR ($CDCl_3$), δ 1.57 (s, 6H). Anal. Calcd. for $C_5H_6N_2O_2Cl_2$ (197.03): C 30.47; H 4.64; N 14.21%. Found: C 30.48; H 3.04; N 13.92%.

Kinetic Studies. All the kinetic measurements were performed at 25± 0.1 ℃ on a Shimadzu MPS-500 UV-spectrophotometer. All the buffers were prepared from doubly distilled water. The stock solutions (4×10^{-3} M) of PNPA and PNPDPP were prepared in dry dioxane. The stock solutions (1.7×10^{-1} M) of C_4-DCI, C_6-DCH, and $2C_1$-DCH were prepared in dry dioxane, while that of DCI was prepared in distilled water. All of the stock solutions were preequilibrated at 25± 0.1 ℃ for 15 min. before each kinetic run. Hydrolysis reactions were initiated by injecting 30 μL of PNPA or PNPDPP stock solution into 3 mL of micellar surfactant solution which contained 20 μL of the catalyst stock solution. The reactions were monitored at 400 nm for the absorbance of 4-nitrophenolate. The rate constants were calculated by pseudo-first order kinetics or series first-order kinetics, and their correlation coefficients were >0.98.

Isolation of 2,6-dibromo-4-nitrophenol. 5.5 g of CTABr was dissolved in 150 mL of DI water and added by 2 g (96 mmol) of DCI at 25 ℃. The color of the solution turned yellow immediately. After 2 min, 1 g of *p*-nitrophenol (48 mmol) was added and stirred for 40 min. After 10 g of $NaHSO_4$ was added, 100 mL of acetonitrile was added, saturated by $MgSO_4$. The upper layer of acetonitrile solution was separated and evaporated to dryness, which was dissolved in ethyl acetate, washed with 1 N HCl (3x), evaporated, and crystallized in ethanol/water. Yield 212 mg (9%); mp 126-128 ℃; TLC, Rf 0.7 ($CHCl_3$: MeOH : AcOH = 8 : 8 : 2, v/v); Anal. Cacld. for $C_6H_3N_1O_3Br_2$ (296.90): C 24.27; H 1.02; N 4.72%. Found: C 24.55; H 1.12; N 4.63%.

References

1. (a) Menger, F. M.; Whitesell, L. G. *J. Am. Chem. Soc.* **1985**, *107*, 707. (b) Moss, R. A.; Kim, K. Y.; Swarup, S. *ibid.* **1986**, *108*, 788. (c) Menger, F. M.; Gan, L. H.; Johnson, E.; Durst, D. H. *ibid.* **1987**, *109*, 2800. (d) Mackay, R. A.; Longo, F. R.; Knier B. L.; Durst, H. D. *J. Phys. Chem.* **1987**, *91*, 861. (e) Moss, R. A.; Ganguli, S. *Tetrahedron Lett.* **1989**, *30*, 2071. (f) Lee, Y. H.; Park, H.; Choi, K. N.; Chang, S. I.; Kim, T. H. *J. of Korean Ind. & Eng. Chemistry* **1994**, *5*, 114.
2. Park, B. D.; Lee, Y. S. *Bull. Korean. Chem. Soc.* **1992**, *13*(1), 5.
3. Park, B. D.; Lee, Y. S. *ibid.* **1992**, *13*(4), 357.
4. Bucherer, H. T.; Lieb, V. A. *J. Prakt. Chem.* **1934**, *141*(2), 5.
5. Frost, A. A.; Pearson, R. G. Kinetics and Mechanism; 2nd ed., Wiley: New York, 1961, pp 166-169.
6. Smith, M. A.; Applegate, V. C.; Johnson, B. G. H. *J. Chem. Eng. Data* **1961**, *6*, 607.
7. Rook, J. J. *Environ. Sci. & Technol.* **1977**, *11*, 478.
8. Soulard, M.; Block, F.; Hatterrer, A. *J. Chem. Soc. Dalton Trans.* **1981**, 2300.
9. Kumar, K.; Margerum, D. W. *Inorg. Chem.* **1987**, *26*, 2706.
10. (a) Mills, J. F.; Schneider, J. A. *Ind. End. Chem. Prod. Res. Dev.* **1973**, *12*, 160. (b) Jolly, R. L. Water Chlorination Environmental Impact and Health Effects; Ann Arbor Sci. **1975**, pp 21-77. (c) Voudrias, E. A.; Reinhard, M. *Environ. Sci. & Technol.* **1988**, *22*, 1049.
11. Minato, H.; Takeda, K.; Miura, T.; Kobayashi, M. *Chem. Letter* **1977**, 1095.
12. Kurz, J. L. *J. Phys. Chem.* **1962**, *66*, 2239.

Crystal Geometry Optimization of β-Lactam Antibiotics Using MMFF Parameters

Youngdo Won

Department of Chemistry, Hanyang University, Seoul 133-792, Korea

Received June 26, 1995

A generic force field approach has been applied to geometry optimization of penam and cephem crystals. The crystalline state energy and force evaluation with the universal force field (MMFF : Merck Molecular Force Field) results in good agreements with the crystallographic data. Bond lengths are usually correct to within 0.02 Å and bond angles usually to within 2.5° The conformation of the β-lactam bicyclic rings in the crystal environment is also well reproduced. The results thus demonstrate the applicability of MMFF to modeling of newer molecular constructs in condensed phase.

Introduction

Since the molecular mechanics (MM2) force field was first introduced by Allinger in the late 1970s,[1] there have been concentrated efforts in optimizing transportable force fields suitable for simulations of liquid states and complex macromolecular assemblies. Among the most widely used are the MM2[1,2] and MM3[3] force fields useful for studying a variety of organic and inorganic systems and the AMBER (Assisted Model Building with Energy Refinement) force fields[4] of Kollman and co-workers and the CHARMM (Chemistry at HARvard Macromolecular Mechanics) force fields[5] of Karplus and co-workers for proteins and nucleic acids.

Despite these efforts, one often encounters the problem of "missing parameters" in a routine computational chemistry application dealing with new molecular moieties. The molecular construct could be a newly designed receptor or a potent therapeutic agent. Because it is not clear how to generalize force field parameters for similar atoms in slightly different environments, one has to develop a suitable parameter set for the new molecule and thoroughly check its validity in one's intended research, which is a time consuming and challenging procedure.

In order to facilitate molecular modeling research of molecular systems with little or no experimental data available (and as a consequence, with no readily available force field parameters), a few generic force fields have been considered: DREIDING of Goddard and co-workers,[6] UFF (Universal Force Field) of Rapp and co-workers,[7] VALBOND of Landis and co-workers[8] and MMFF (Merck Molecular Force Field) of Halgren and co-workers.[9] The generic force fields have certain advantages in dealing with new molecular constructs that have never been parameterized, because they can theoretically cover the entire periodic table. Inorganic systems including transition metals as well as macromolecular systems with the molecular structure far from equilibrium can be easily modeled with the generic force fields.

In this work, we have optimized several penam and cephem crystals using the most recent MMFF parameter set. Penicillins and cephalosporins are β-lactam antibiotics that inhibit the transpeptidases and carboxypeptidases involved in the biosynthesis of the peptidoglycan bacterial cell walls.[10] The biological activity of these compounds is strongly related to the reactivity of the β-lactam ring.[11] For the ratio-